Available online at www.sciencedirect.com
SCIENCE DIRECT®
Journal of Non-Crystalline Solids 334&335 (2004) 270–275
JOURNAL OF NON-CRYSTALLINE SOLIDS
www.elsevier.com/locate/jnoncrysol

Synthesis and devitrification of glassy Zr–Ti–Ni and Zr–Hf–Ni ternary alloys

Joysurya Basu [a,*], D.V. Louzguine [b], A. Inoue [b], S. Ranganathan [a]

[a] Department of Metallurgy, Indian Institute of Science, Bangalore 560012, India
[b] Institute for Materials Research, Tohoku University, Katahira 2-1-1, Aoba-ku, Sendai, Japan

Abstract

Two alloys of nominal compositions $Zr_{41.5}Ti_{41.5}Ni_{17}$ and $Zr_{41.5}Hf_{41.5}Ni_{17}$ have been melt spun at 40 ms^{-1} wheel speed. Under this processing condition Zr–Ti–Ni alloy becomes amorphous and the Zr–Hf–Ni alloy precipitates a cubic phase with 4.95 Å lattice parameter in the amorphous matrix. The Zr–Ti–Ni alloy, upon annealing, precipitates a nanoquasicrystalline phase, which at the later stages of crystallisation transforms into cF96 $NiZr_2$ phase. The amorphous phase in Zr–Hf–Ni alloy upon annealing precipitates the same cubic phase with 4.95 Å lattice parameter. The lower glass forming ability of Zr–Hf–Ni compared to Zr–Ti–Ni and nanoquasicrystallisation in Zr–Ti–Ni alloy can be explained by taking into consideration the atomic size differences among Ti, Zr and Hf.

PACS: 81.07.Bc; 61.44.Br; 61.43.Fs; 61.66.Dk

1. Introduction

Since the discovery of bulk metallic glasses, Zr based alloys have been studied most intensively [1]. These alloys can be classified into two groups depending on the alloying constituents. One class is Zr and Al with transition metals in which Cu and Ni are very important alloying additions. The second class of alloys is synthesised with transition metals without Al. In the latter category of alloys Zr can be partially or fully replaced by Hf and Ti to obtain quaternary and higher order alloys. The addition of Pd, Pt, Au and Ag introduces changes in their thermal stability [2]. In the (Zr, Hf, Ti)–Ni system, it is possible to design three binary, three ternary and one quaternary alloy systems. In binary alloys of Zr, Hf and Ti with Ni, glasses form over a wide composition range, as there are a number of deep eutectics and intermetallic compounds in the phase diagrams [3,4]. In the ternary alloys, Ti–Zr–Ni is the most widely studied system. Both metastable and stable quasicrystals have been reported to occur in this system depending upon the processing conditions [5–7]. Annealing at higher temperatures gives rise to the 1/1 approximant phase. The phase transformation of this alloy system is complex and all these transformations can be avoided to produce an amorphous phase by non-equilibrium processing techniques [8]. In Ti–Hf–Ni system a similar quasicrystal and a rational approximant have been reported [9,10]. The Zr–Hf–Ni system has not received much attention in this context. Indeed this system is likely to show a very different behaviour as for all practical purposes the entire ternary diagram can be treated as pseudo-binary sections, as many binary intermetallics are common to Zr–Ni and Hf–Ni systems.

Though there are a large number of reports on nanocrystallisation and nanoquasicrystallisation in Zr based alloys, the structural origin of nanoquasicrystals and structurally complex intermetallic phases is still not properly understood. A complete understanding of the glass formation and crystallisation behaviour of ternary (Ti, Zr, Hf)–Ni alloys will be helpful in rationalising the behaviour of other alloys. The aim of this work is to investigate the glass forming and quasicrystal forming ability of Zr–Ti–Ni and Zr–Hf–Ni ternary alloys and to understand the effect of the substitution of titanium by hafnium in a Zr–Ti–Ni alloy.

* Corresponding author. Tel./fax: +91-080-3601198.
E-mail address: surya@platinum.metalrg.iisc.ernet.in (J. Basu).

0022-3093/$ - see front matter © 2004 Elsevier B.V. All rights reserved.
doi:10.1016/j.jnoncrysol.2003.11.055

2. Experimental techniques

Two alloys of nominal composition $Zr_{41.5}Ti_{41.5}Ni_{17}$ and $Zr_{41.5}Hf_{41.5}Ni_{17}$ (compositions are expressed in at%) have been investigated. Pure Zr (99.99%), Ti (99.99%), Hf (99.99%) and Ni (99.9%) were taken in proper proportion and they were melted in a vacuum arc melting furnace with back filled argon gas. The alloys were melted several times in order to ensure the compositional homogeneity. Then the alloys were melt spun in a single roller melt spinning unit at a wheel speed of 40 ms^{-1} in an argon atmosphere. The melt spun ribbons are approximately 5 mm in width and 50–60 μm in thickness. The melt spun ribbons were characterised with a JEOL 8030 X-ray diffractometer using Cu Kα radiation and a JEOL 2000 FX II transmission electron microscope. The thermal stability and the transformation behaviour of the alloys were studied with a DSC 822E Mettler Toledo differential scanning calorimeter. In order to study the phase evolution, the ribbons were annealed at the peak temperatures as indicated by the DSC and in the supercooled liquid region for 10 min and 4 h. Before heat treatment the samples were encapsulated in a quartz tube under vacuum. The heat treated samples were characterised by X-ray diffraction and transmission electron microscopy.

3. Results

X-ray diffraction patterns of the Zr–Ti–Ni and Zr–Hf–Ni alloys, melt spun at 40 ms^{-1} wheel speed, are given in Fig. 1. In the diffraction pattern of the Zr–Ti–Ni alloy no peak corresponding to any crystalline phase is seen. A diffuse diffraction hump over the angular range 30°–40° confirms the presence of an amorphous phase in the melt spun ribbon. In the diffraction pattern of the Zr–Hf–Ni alloy one sharp peak can be seen. The peak cannot be indexed to any known crystalline phase with certainty. The transmission electron micrograph and diffraction pattern of the Zr–Ti–Ni and Zr–Hf–Ni alloy is given in Fig. 2(a) and (b) respectively. In the Zr–Ti–Ni alloy no crystalline phase can be seen and the presence of the amorphous phase can be confirmed from the diffraction halo. The microstructure of the Zr–Hf–Ni alloy after melt spinning is not uniform. Though a considerable amount of amorphous phase is present in the ribbon, densely populated crystallites can be seen in localised regions. The precipitates are dendritic in nature and their size varies in the range of 50–100 nm. A convergent beam electron diffraction pattern with a large spot size is given in Fig. 2(b), inset. In the diffraction pattern a faint diffuse halo confirms the presence of the amorphous phase. The spots in the diffraction pattern conform to the [0 0 1] pattern of an FCC phase. The lattice parameter of the phase is 4.95 Å. This observation substantiates the fact that the alloy after melt spinning is not totally amorphous and the microstructure is inhomogeneous in nature. Due to this inhomogeneity, the presence of the amorphous phase is masked in the X-ray diffraction pattern. The peaks in the X-ray diffraction pattern can also be indexed as FCC by taking 4.95 Å lattice parameter.

Differential scanning calorimetric thermograms of the Zr–Ti–Ni and Zr–Hf–Ni alloy are shown in Fig. 3. The Zr–Ti–Ni alloy crystallises in three exothermic heat events. The peak temperatures for the thermal events are 810, 880 and 930 K. These temperatures and 700 K (in

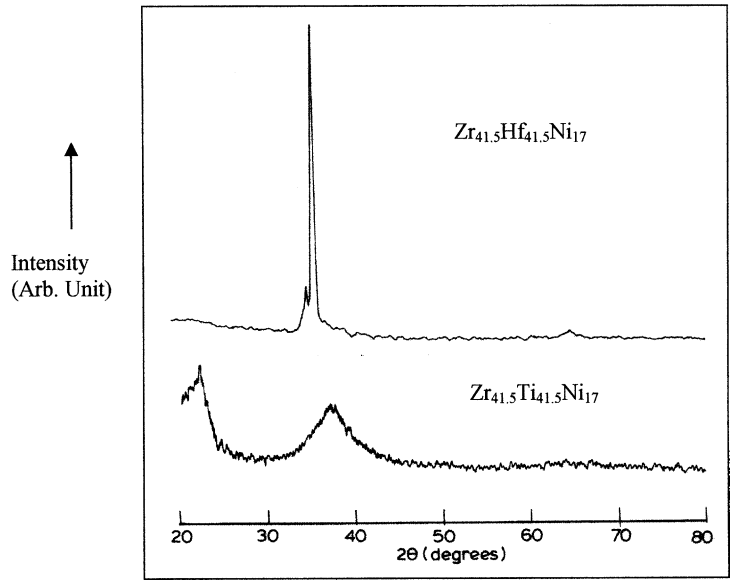

Fig. 1. X-ray diffraction patterns of $Zr_{41.5}Hf_{41.5}Ni_{17}$ and $Zr_{41.5}Ti_{41.5}Ni_{17}$ alloy melt spun at 40 ms^{-1} wheel speed.

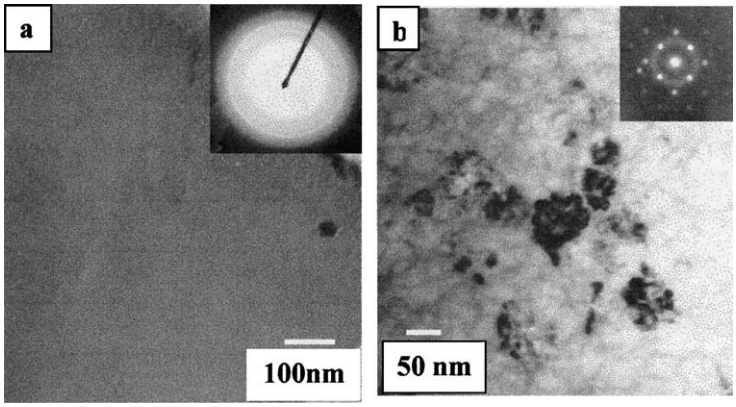

Fig. 2. Transmission electron micrograph and electron diffraction pattern (inset) for (a) Zr–Ti–Ni (b) Zr–Hf–Ni alloy after melt spinning at 40 ms^{-1} wheel speed. In the Zr–Hf–Ni alloy presence of crystalline phases in the amorphous matrix can seen.

the supercooled liquid region) were taken as the annealing temperatures. The thermogram of the Zr–Hf–Ni alloy reveals that the alloy crystallises in a single exothermic heat event though a small diffuse exothermic hump is seen just before the main crystallisation event. The peak temperature for the reaction is 728 K. So the melt spun alloy was annealed at 653 K (below the first crystallisation temperature) and 728 K in order to study the phase evolution during crystallisation.

The transmission electron micrograph and the diffraction patterns of the Zr–Ti–Ni alloy annealed at 810 K for 10 min are given in Fig. 4(a)–(d). In the micrograph fine precipitates varying in the size range of 40–60 nm are distributed in the amorphous matrix. The precipitates are almost spherical in shape. The nano beam electron diffraction patterns from the precipitates reveal the quasicrystalline nature with icosahedral symmetry. The fivefold, threefold and twofold patterns are shown respectively in the Fig. 4(b)–(d). The alloy precipitates an icosahedral quasicrystalline phase after heat treatment at 700 K. After heat treatment at 810 K the volume fraction of the quasicrystalline phase increases and their size remains almost the same. Transmission electron micrograph and the convergent beam electron diffraction pattern of the alloy annealed at 880 K are given in Fig. 5. After this heat treatment the grains grow in size from 100 to 300 nm. The grains are faceted and polygonal in shape. At this stage the presence of the quasicrystalline phase cannot be seen. Convergent beam electron diffraction pattern along the cubic [0 0 1] zone axis, given in the inset reveals the presence of cF96 $Ni(Zr\ Ti)_2$ phase. There is another $NiZr_2$ phase which is tI12 with the structure of Al2Cu. The presence of this phase can also be confirmed at this stage. The phase evolution sequence in this alloy remains the same after 10 min and 4 h of annealing. This observation indicates that the phases are stable at the temperature of annealing up to 4 h. Even after 4 h of annealing grain growth is not significant.

The Zr–Hf–Ni alloy starts crystallising below the first exothermic heat event. After heat treatment at 653 K the volume fraction of the cubic phase in the alloy increases and the size of the precipitates varies in the range of 50–100 nm. A transmission electron micrograph of the alloy annealed at 728 K is shown in Fig. 6. In the micrograph two different morphological types of precipitates can be

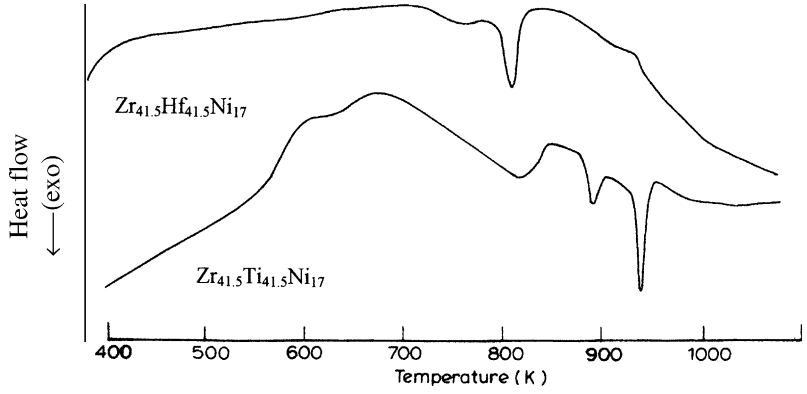

Fig. 3. Differential scanning calorimetric thermograms of the Zr–Hf–Ni and the Zr–Ti–Ni alloy melt spun at 40 ms^{-1} wheel speed.

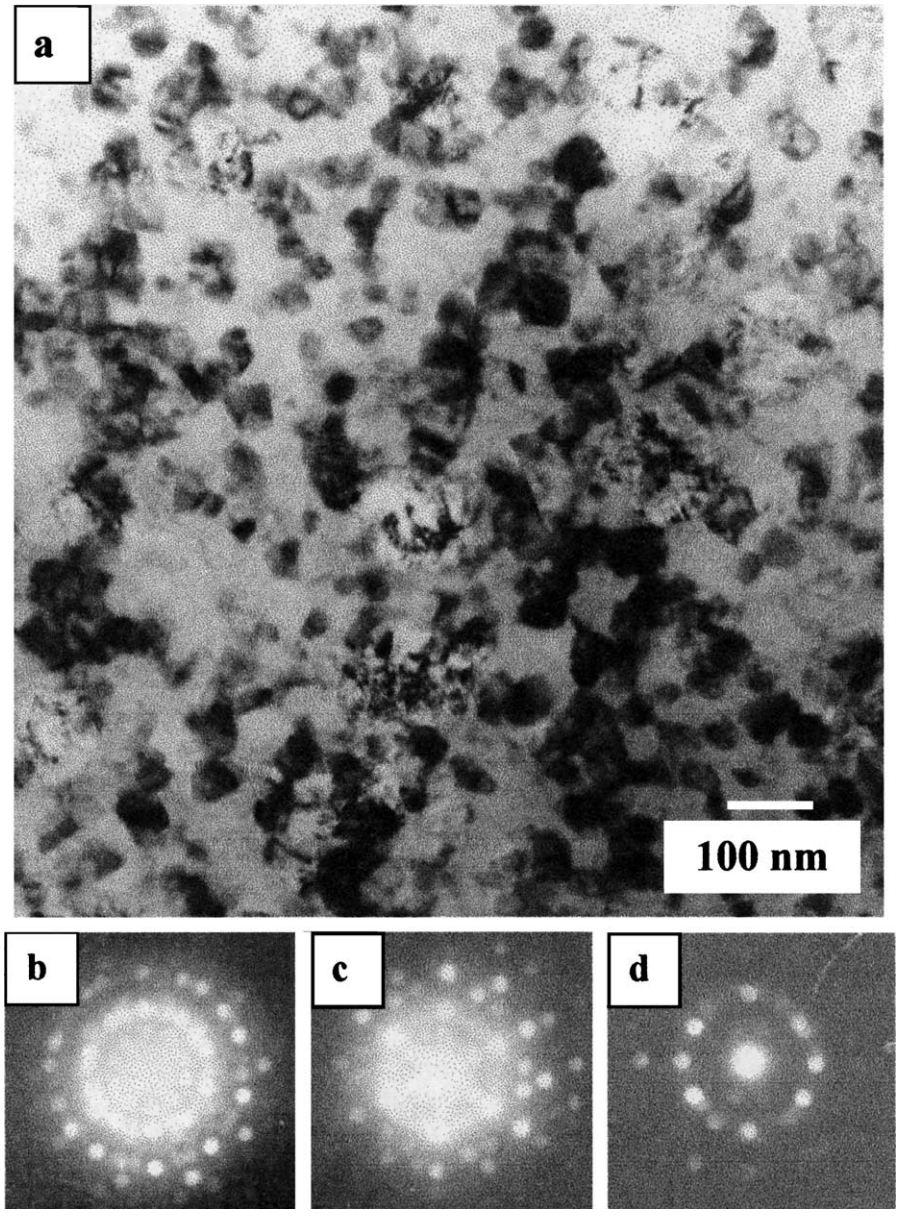

Fig. 4. Transmission electron micrograph of the Zr–Ti–Ni melt spun alloy annealed at 810 K for 10 min (b) fivefold (c) threefold (d) twofold electron diffraction patterns from the precipitates showing the presence of icosahedral quasicrystalline phase.

seen. One kind of precipitate is spherical or polygonal in shape and the other type exhibits a mottled contrast. The nano beam electron diffraction pattern along the [1 1 1] axis (Fig. 6 inset) from the polygonal precipitates reveals the presence of the same cubic phase with a 4.95 Å lattice parameter. This does not match with any of the known intermetallics in the relevant systems and needs further investigation.

4. Discussion

Zr–Ti–Ni and Zr–Hf–Ni alloys in the present study are synthesised under the same experimental conditions. While the Zr–Ti–Ni alloy amorphises completely but the Zr–Hf–Ni alloy shows localised precipitation of a cubic phase. The precipitation of a similar cubic phase has been reported in earlier work on Hf–Ni–Cu–Al–Ti alloy with a lattice parameter of 5.3 Å [11]. It is not confirmed in this study whether these two phases with different lattice parameters arise from a similar intermetallic.

Though Ti, Zr, and Hf appear in the same group in the periodic table, the replacement of Ti by Hf reduces the glass forming ability of the alloy. Though the heat of mixing of Ti, Zr and Hf with Ni is highly negative, the atomic radii mismatch between Zr and Hf is considerably lower than that between Zr and Ti (Table 1). So the replacement of Ti by Hf does not really add to the glass

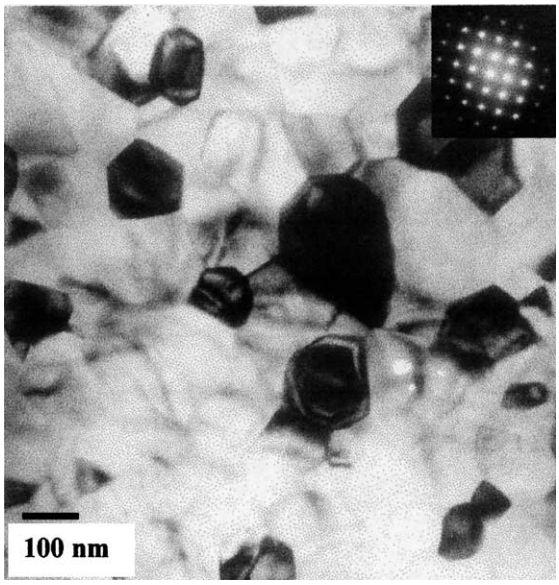

Fig. 5. Transmission electron micrograph of the Zr–Ti–Ni melt spun alloy annealed at 880 K. Inset [0 0 1] Electron diffraction pattern from the cubic $NiZr_2$ phase.

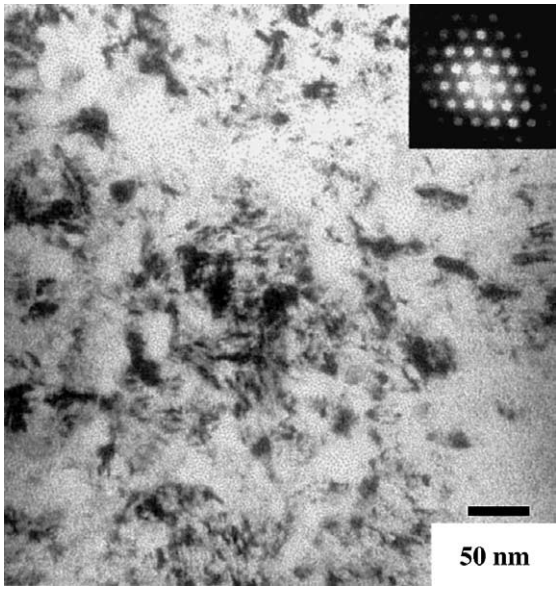

Fig. 6. Transmission electron micrograph of the Zr–Ti–Ni melt spun alloy annealed at 728 K. Inset [1 1 1] electron diffraction pattern from the cubic phase.

forming ability. This fact can further be qualitatively substantiated by binary and ternary phase diagrams. All three binary diagrams Ti–Ni, Zr–Ni and Hf–Ni feature deep eutectics. It is also noteworthy that Zr–Ni and Hf–Ni alloys form many more intermetallics than Ti–Ni, indicating the close similarity between Zr and Hf and the difference with Ti. This is mainly because of the larger size difference between Zr and Hf with Ti. In the ternary Zr–Ti–Ni phase diagram a number of intermetallics can be seen and in the central region which is very close to the present composition, low melting phases exist. In the vertical section of $NiTi_2$–$NiZr_2$, which also goes through the low melting region, eutectics can be seen. A similar trend exists with Ti–Hf–Ni system [9,10]. The ternary diagram for Zr–Hf–Ni is not available. A clear understanding of this ternary phase diagrams may help in explaining the lower glass forming ability of Zr–Hf–Ni alloy.

Table 1
Atomic radii mismatch and heat of mixing between Ti, Zr, Hf with Ni

Atomic radii/mismatch ΔH_{mix} kJ/mole	Zr	Ti	Hf	Ni
Zr		9%	1%	22%
Ti	0		7%	15%
Hf	0	0		21%
Ni	−49	−35	−42	

The crystallisation behaviour of the two alloys is again different. The Zr–Ti–Ni alloy upon heat treatment in the supercooled liquid region and at the first crystallisation temperature precipitates icosahedral quasicrystals which upon further high temperature heat treatment transform into the cF96 $Ni(Zr\ Ti)_2$ phase. The quasicrystalline phase is stable up to 4 h of annealing treatment at the peak temperature as indicated by the DSC. The Zr–Hf–Ni alloy after melt spinning precipitates a cubic phase with 4.95 Å lattice parameter in the amorphous matrix. The amorphous phase upon crystallisation precipitates the same phase.

The occurrence of a ternary hexagonal Laves phase has been reported in both Ti–Zr–Ni and Ti–Hf–Ni systems [12,13]. In the binary alloys of these metals a Laves phase does not occur. In ternary alloys the combination of elements with different sizes favours the formation of Laves phase, Again in Zr–Hf–Ni system it is inferred that such a Laves phase does not occur.

It is concluded that in the three homologous systems of Ti–Zr–Ni, Ti–Hf–Ni and Zr–Hf–Ni the first two are very similar with high glass, quasicrystal and topologically closepacked Laves phase forming ability mainly due to the size difference between Zr and Hf on the one hand and Ti on the otherhand. In the third ternary system the close size of Zr and Hf precludes this and leads to a lowering of glass forming ability and the non-occurrence of both quasicrystals and Laves phases.

5. Conclusions

Though Ti, Zr and Hf belong to the same group in the periodic table, they affect the glass forming ability of the alloy differently. Nanoquasicrystallisation is observed in Zr–Ti–Ni alloy, whereas nanocrystallisation is observed in Zr–Hf–Ni alloy. The difference in crystallisation behaviour can be explained on the basis of the

atomic size of the elements. Nanoquasicrystallisation is enhanced as the atomic radii mismatch reaches nearer to the ideal value, i.e. 10%.

Acknowledgements

The authors would like to acknowledge stimulating discussions and with Professor K. Chattopadhyay, Professor V. Jayaram, Professor B. S. Murty and Dr U. Ramamurty in course of this work. Research funding from Board of Research in Nuclear Sciences (DAEO/MMT/SRG/105) is gratefully acknowledged.

References

[1] A. Inoue, C. Fan, J. Saida, T. Zhang, Sci. Tech. Adv. Mater. 1 (2000) 73.
[2] A. Inoue, T. Zhang, J. Saida, M. Matsushita, M.W. Chen, T. Sakurai, Mater. Trans. JIM 40 (1999) 1181.
[3] D.E. Polk, A. Calka, B.C. Giessen, Acta. Met. 26 (1978) 1097.
[4] Z. Altounian, T. Guo-hua, J.O. Strom-Olsen, J. Appl. Phys. 54 (1983) 3111.
[5] V.V. Molokanov, V.N. Chebotnikov, J. Non-Cryst. Solids 117&118 (1990) 789.
[6] K.F. Kelton, W.J. Kim, R.M. Stroud, Appl. Phys. Lett. 70 (1997) 3230.
[7] S. Yi, D.H. Kim, J. Mater. Res. 15 (2000) 892.
[8] G.W. Lee, T.K. Croat, A.K. Gangopadhyay, K.F. Kelton, Philos. Mag. Lett. 82 (2002) 199.
[9] Y.K. Kovonoristyi, V.N. Chebotnikov, Y.K. Mukhina, Proc. Ninth International Conference on Rapidly Quenched and Metastable Materials, Elsevier, Amsterdam, 414.
[10] V.T. Huett, K.F. Kelton, Phil. Mag. Lett. 82 (2002) 191.
[11] C. Li, J. Saida, M. Matsushita, A. Inoue, Philos. Mag. Lett. 80 (2000) 621.
[12] V.V. Molokanov, V.N. Chebotnikov, Y.K. Kovneristyi, Inorganic Mater. 25 (1989) 46.
[13] E.L. Semenova, L.A. Tretyachenko, Powder Metall. Metal Ceram. 40 (2001) 414.